Journal of Theoretical and Applied Information Technology
30th April 2013. Vol. 50 No.3

ISSN: 1992-8645 www.jatit.org E-ISSN: 1817-3195

CROSSTALK ANALYSIS FOR HIGH-PRECISION OPTICAL PICKUP ACTUATOR SYSTEM

QINGXI JIA, *ZHIZHENG WU, YANG LI, MEI LIU

Department of Precision Mechanical Engineering,

Shanghai University, Shanghai, China, 200072

*E-mail: zhizhengwu@shu.edu.cn

ABSTRACT

The traditional optical pickup actuator model based on the assumption that the actuator spatial magnetic field distributes uniformly ignores the crosstalk characteristic among the movements of different directions. Crosstalk characteristic is a key factor that affects the actuator dynamic property and, consequently, the accuracy of reading and writing operation in the future higher density optical storage systems. In this paper, the actuator spatial magnetic field distribution model is first established, then the crosstalk movement phenomenon of the actuator is analyzed and simulated in CST software based on finite-difference time-domain (FDTD) principle. By investigating the parameters of the width and height of the permanent magnet and the thickness of the focusing coil, it is concluded that the crosstalk characteristic is closely related with these structural parameters and crosstalk can be effectively reduced by optimal design of them, thus, the dynamic performance of the actuator can be improved.

Keywords: *Crosstalk Characteristic, Optical storage, Higher density, Structural Parameters*

1. INTRODUCTION

With the density of optical disk storage and data transfer speed continuing to increase, the requirements of the actuator movement accuracy and dynamic performance in high-precision optical storage systems become higher and higher. The distance between the objective lens and disc will drop down to less than 100 *nm* for the next generation near field optical storage systems[1], which necessitates a even demanding position accuracy. Crosstalk characteristic between each movement direction in the traditional pickup actuators not only results in the declining of the reading and writing accuracy, but also could cause a collision between the objective lens and the disk.

In the two-dimensional actuator as shown in Figure 1, the movable parts are supported by both the suspension wires and the electromagnetic force and perform the two-dimensional movements, including focusing movement and tracking movement. The focusing movement makes the objective lens move in the direction perpendicular to the optical disc surface to ensure the focusing spot focusing on the disc surface accurately. Tracking movement can effectively control the objective lens to move in the direction parallel to the optical disc surface [2].

Assuming the actuator spatial magnetic field distributes uniformly, the traditional actuator model simply considers the movements of the tracking and focusing directions separately and therefore the crosstalk characteristic between each movement is ignored. Since the focusing and tracking movements follow the same principle in the low frequency range, the movement in each direction usually is simplified as a one-dimensional mass-spring-damper system, as shown in Figure 2[3-4]. However, this traditional model based on the uniform magnetic field is no longer applied in the future higher density optical storage system. In this paper the non-uniform magnetic field and the cross-force applied to the movable components of actuator are analyzed, and the crosstalk characteristic is further simulated in CST software based on FDTD principle.

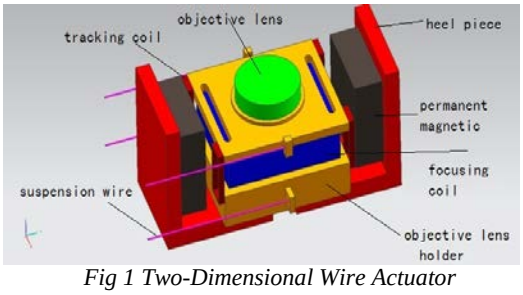

Fig 1 Two-Dimensional Wire Actuator

Journal of Theoretical and Applied Information Technology
30th April 2013. Vol. 50 No.3

ISSN: 1992-8645 www.jatit.org E-ISSN: 1817-3195

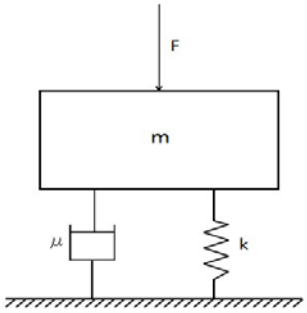

Fig. 2 One-Dimensional Mass-Spring-Damper System Model

2. SPATIAL MODEL OF MAGNETIC FIELD

The force on the actuator is decided by the distribution of the electromagnetic field. Therefore, the analysis of the electromagnetic field is critical to optimize the dynamic characteristic of the actuator[5-7]. Generally, the two-dimensional wire actuator's spatial magnetic field is mainly composed of a magnetic field generated by two permanent magnets, a magnetic field generated by the focusing coil and a magnetic field generated by the four tracking coil, as shown in Figure 3. In initial state, the permanent magnets, the focus coil and tracking coil share one geometric center denoted as point $O_i(x_i, y_i, z_i)$. When they move away from the central location, their geometric centers will be denoted as $O_i(x_i, y_i, z_i)$、$O_f(x_f, y_f, z_f)$、$O_t(x_t, y_t, z_t)$, respectively.

2.1 SPATIAL MAGNETIC FIELD MODEL OF PERMANENT MAGNET

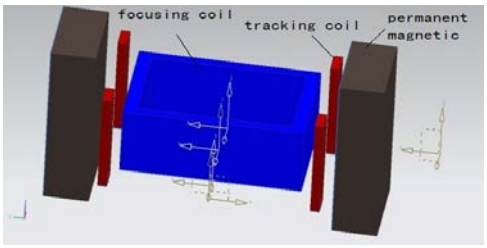

Fig. 3 Diagram Of The Actuator Coils

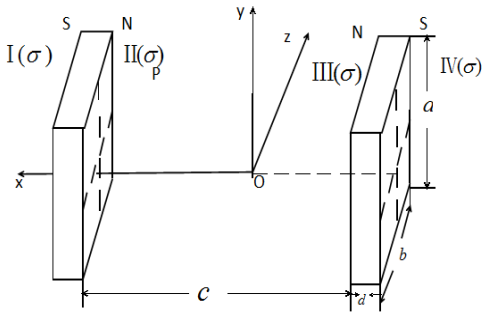

Fig. 4 Actuator Permanent Magnetic

According to the theory of medium magnetization, $-\nabla\mu_0 \cdot M$ was regarded as a hypothetical magnetic charge density while computing the magnetic field of the permanent magnet. In the permanent magnet which is magnetized uniformly, surface charge only exit on the interface of magnetic medium. Surface magnetic charge density σ is

$$\sigma = \mu_0 \vec{M} \cdot \vec{n} \tag{1}$$

The permanent magnet actuator is shown in Figure 4. Assuming the permanent magnets are uniformly magnetized, the two opposite surfaces Ⅱ、Ⅲ are magnetized as N pole, the other two surfaces Ⅰ and Ⅳ are magnetized as S pole. According to the equivalent magnetic charge method, unit magnetic charge at the point $P_1(x_1, y_1, z_1)$ on the surface generates magnetic flux at any point in the space. The magnetic induction of any point $P(x, y, z)$ generated by the point $P_1(x_1, y_1, z_1)$ on the surface Ⅰ, can be expressed as:

$$d\vec{B}_1 = \frac{1}{4\pi}\frac{\sigma\vec{r}_1}{r_1^3}dA_1 \tag{2}$$

where $\vec{r}_1 = (x-x_1)\vec{i} + (y-y_1)\vec{j} + (z-z_1)\vec{k}$ can be computed according to the magnetic field superposition principle. dA_1 is the surface integral to surface Ⅰ. Magnetic field distribution generated by surface Ⅰ is:

$$\begin{aligned}\vec{B}_1 &= \frac{1}{4\pi}\int_{m_1}^{m_2}\int_{n_1}^{n_2}\frac{\vec{r}_1\sigma dy_1 dz_1}{r_1^5} \\ &= \frac{\sigma}{4\pi}\int_{m_1}^{m_2}\int_{n_1}^{n_2}\frac{(x-x_1)\vec{i} + (y-y_1)\vec{j} + (z-z_1)\vec{k}}{r_3^5}dydz\end{aligned} \tag{3}$$

where

$m_1 = y_i - a_i/2,\ m_2 = y_i + a_i/2,\ n_1 = z_i + b_i/2,\ n_2 = z_i + b_i/2.$

The magnetic field generated by the permanent magnet is the sum of the four magnetic field generated by the surfaces Ⅰ, Ⅱ, Ⅲ and Ⅳ

$$\vec{B}_i = \sum_{n=1}^{4}\vec{B}_n = B_{ix}\vec{i} + B_{iy}\vec{j} + B_{iz}\vec{k} \tag{4}$$

Denote $\iint_F = \int_{m_1}^{m_2}\int_{n_1}^{n_2}$, $d_A = d_y d_z$, $w = x, y, z$, F Ⅰ、Ⅱ、Ⅲ、Ⅳ, then

$$B_w = \frac{\sigma}{4\pi}\sum_{n=1}^{4}\iint_F\frac{(x-x_n)}{r_n^5}dA_n \tag{5}$$

Journal of Theoretical and Applied Information Technology
30th April 2013. Vol. 50 No.3

ISSN: 1992-8645 www.jatit.org E-ISSN: 1817-3195

2.2 Spatial Magnetic Field Model Of Focusinging Coil

Coils of actuator are wounded by excellent conductor. The analysis can be performed according to the electromagnetic field produced by the current source.

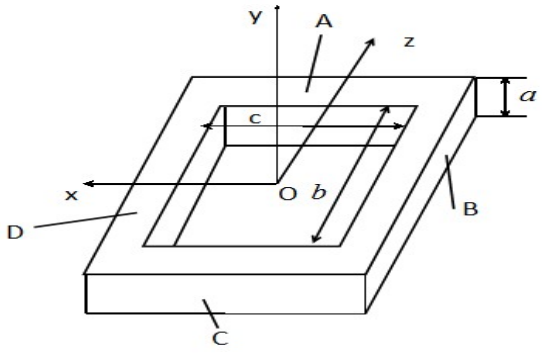

Fig.5The Structure Of The Focusing Coil

Biot-Savart law states that the magnetic induction d_B of any point p generated by the current element $\boldsymbol{I\,dl}$ is proportional to the current element, and proportional to the sine of the angle θ between the current element $\boldsymbol{I\,dl}$ and the vector r from the current element to the point of p, and inversely proportional to the square of the size of the vector:

$$dB = \frac{\mu_0}{4\pi}\frac{I\,dl\sin\theta}{r^2} \tag{6}$$

The vector expression is as follows:

$$d\vec{B} = \frac{\mu_0}{4\pi}\frac{\vec{I}\times\vec{r}}{r^3}dV \tag{7}$$

where, $\frac{\mu_0}{4\pi}$ is a proportional coefficient, μ_0 is the permeability of vacuum, and its value is $\mu_0 = 4\pi\times10^{-7}\,N\cdot A^{-2}$.

The structure of the focusing coil is shown in the Figure 5. The height, width and length of focusing coil are denoted as a_f、b_f、c_f respectively .The turns of the focusing coil is n_f, the diameter of the coil wire is d_f, and the input current is I_f. The coil is equivalent to a uniform annulus loop. The equivalent current density is $J_f = 4I_f/\pi d_f^{\,2}$ and the equivalent current thickness is $T_f = \pi n d_f^{\,2}/4n_f$. The coil is divided into four parts called A, B, C and D. Each part of the current is uniform. Taking C segment for example, the magnetic field generated by the current element at any point is:

$$\begin{aligned} d\vec{B}_c &= \frac{\mu_0}{4\pi}\frac{J_f\vec{r}\times\left[(y-y_c)\vec{j}+(z-z_c)\vec{k}\right]}{r_c^3}dV_c \\ &= \frac{\mu_0 J_f}{4\pi}\frac{(y-y_c)\vec{k}-(z-z_c)\vec{j}}{r_c^3}dV_c \end{aligned} \tag{8}$$

then,

$$\vec{B}_c = \frac{\mu_0 J_f}{4\pi}\iiint_V \frac{(y-y_c)\vec{k}-(z-z_c)\vec{j}}{r_c^3}dV_c \tag{9}$$

where dV_c is volume integral to part C.

The expression of the magnetic field generated by the other three coils can be obtained in the same way. Then the superposition principle can be applied to obtain the total spatial magnetic field generated by the focusing coils:

$$\vec{B}_f = \sum_{i=1}^{4}\vec{B}_i = B_{fx}\vec{i} + B_{fy}\vec{j} + B_{fz}\vec{k} \tag{10}$$

Therefore, the magnetic field generated by the focusing coil in three directions is:

$$B_{fx} = \frac{\mu_0 J_f}{4\pi}\left[-\iiint_B \frac{y-y_B}{r_B^3}dV_B + \iiint_D \frac{y-y_D}{r_D^3}dV_D\right] \tag{11}$$

$$B_{fy} = \frac{\mu_0 J_f}{4\pi}\begin{bmatrix} -\iiint_A \frac{z-z_A}{r_A^3}dV_A + \iiint_B \frac{x-x_B}{r_B^3}dV_B \\ +\iiint_C \frac{z-z_C}{r_C^3}dV_C - \iiint_D \frac{x-x_D}{r_D^3}dV_D \end{bmatrix} \tag{12}$$

$$B_{fz} = \frac{\mu_0 J_f}{4\pi}\left[\iiint_A \frac{y-y_A}{r_A^3}dV_A - \iiint_C \frac{y-y_C}{r_C^3}dV_C\right] \tag{13}$$

2.3 Spatial Magnetic Field Model Of Tracking Coil

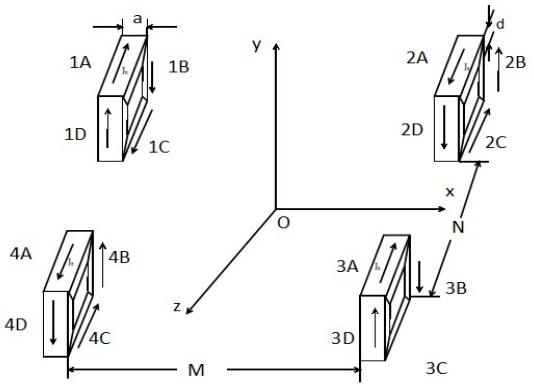

Journal of Theoretical and Applied Information Technology
30th April 2013. Vol. 50 No.3

ISSN: 1992-8645 www.jatit.org E-ISSN: 1817-3195

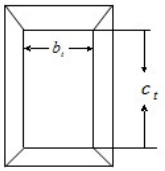

Fig.6 The Structure Of Tracking Coil

The tracking coil structure of the actuator is shown in the Figure 6. With the same definition of the focusing coil, and its structural parameters are considered as the height of the tracking coil (inner circle), the width, the length, and the equivalent thickness of the coil, which are denoted as: L_t、W_t、H_t、n_t, respectively. There are four groups of tracking coils, and each set has n_t turns, with a wire diameter is d_t. The input current is I_t. Similarly, it can be assumed that the respective tracking coils are equivalent to a uniform dense fill rectangular loop. The equivalent of the coil current density is $J_t = 4I_t / \pi d_t^2$, and the equivalent thickness is $T_t = \pi n_t d_t^2 / 4H_t$. Each tracking coil is divided into four parts, and the currents between the adjacent coils are opposite, as shown in the Figure 6:

$$\vec{B}_t = \sum_{n=1}^{4} \vec{B}_{nw} = B_{tx}\vec{i} + B_{ty}\vec{j} + B_{tz}\vec{k} \qquad (14)$$

w represents A, B, C, D, respectively.

The three components of the tracking coil magnetic field are as follows:

$$B_{tx} = \frac{\mu_0 J_t}{4\pi}\{\sum_{i=1,3}[-\iiint_{iA}\frac{y-y_{iA}}{r_{iA}^3}dV_{iA} - \iiint_{iB}\frac{z-z_{iB}}{r_{iB}^3}dV_{iB} + \iiint_{iC}\frac{y-y_{iC}}{r_{iC}^3}dV_{iC} + \iiint_{iD}\frac{z-z_{iD}}{r_{iD}^3}dV_{iD}] + \sum_{j=2,4}[\iiint_{jA}\frac{y-y_{jA}}{r_{jA}^3}dV_{jA} + \iiint_{jB}\frac{z-z_{jB}}{r_{jB}^3}dV_{jB} - \iiint_{jC}\frac{y-y_{jC}}{r_{jC}^3}dV_{jC} - \iiint_{jD}\frac{z-z_{jD}}{r_{jD}^3}dV_{jD}]\} \qquad (15)$$

$$B_{ty} = \frac{\mu_0 J_t}{4\pi}\{\sum_{i=1,3}\left[\iiint_{iA}\frac{x-x_{iA}}{r_{iA}^3}dV_{iA} - \iiint_{iC}\frac{x-x_{iC}}{r_{iC}^3}dV_{iC}\right] + \sum_{j=2,4}\left[-\iiint_{jA}\frac{x-x_{jA}}{r_{jA}^3}dV_{jA} + \iiint_{jC}\frac{x-x_{jC}}{r_{jC}^3}dV_{jC}\right]\} \qquad (16)$$

$$B_{tz} = \frac{\mu_0 J_t}{4\pi}\{\sum_{i=1,3}\left[\iiint_{iB}\frac{x-x_{iB}}{r_{iB}^3}dV_{iB} - \iiint_{iD}\frac{x-x_{iD}}{r_{iD}^3}dV_{iD}\right] + \sum_{j=2,4}\left[-\iiint_{jB}\frac{x-x_{jB}}{r_{jB}^3}dV_{jB} + \iiint_{jD}\frac{x-x_{jD}}{r_{jD}^3}dV_{jD}\right]\} \qquad (17)$$

2.4 The Spatial Total Magnetic Field

Similar to the above analysis for each part, the total magnetic field is also in line with the principle of superposition. The magnetic field at any point $P(x, y, z)$ in the actuator space is as follows:

$$\vec{B}(P) = \vec{B}_i + \vec{B}_f + \vec{B}_t = \sum_i \iint_{A_m}\frac{\sigma_i}{4\pi}\frac{\vec{r}}{r^3}dA_m + \sum_i \iiint_{V_{fi}}\frac{\mu_0}{4\pi}\frac{\vec{J}_{fi}\times\vec{r}}{r^3}dV_{fi} + \sum_i \iiint_{V_{ti}}\frac{\mu_0}{4\pi}\frac{\vec{J}_{ti}\times\vec{r}}{r^3}dV_{ti} \qquad (18)$$

3. THE SIMULATION RESULTS OF THE SPATIAL DISTRIBUTION OF MAGNETIC FIELD

Based on the analysis of spatial magnetic field model, the full results of magnetic field distribution can be observed through numerical simulation. There are a lot of softwares that can be used to calculate the electromagnetic field. The Ansoft from United States based on the finite element analysis and German CST software based on the finite-difference time-domain (FDTD) method are the popular softwares. In this paper, the EM STDIO module of CST software is used to analyze the spatial electromagnetic field of the actuator.

3.1 Simulation Of The Permanent Magnet Field

The spatial magnetic field of the actuator is mainly produced by permanent magnets. In the simulation of the magnetic field of permanent magnets, the material parameters of the geometric model, including relative permeability, remnant flux density and the air relative permeability in the boundary condition, are listed in Table 1.

Table 1 Parameters of permanent magnet

Material	relative permeability	remnant flux density（T）
permanent magnet	1.06	1.4
air	1.0	

Through calculation, the magnetic induction intensity distribution of the permanent magnets in

Journal of Theoretical and Applied Information Technology
30th April 2013. Vol. 50 No.3

ISSN: 1992-8645 www.jatit.org E-ISSN: 1817-3195

the air is displayed in Fig 7and 8. Fig 7 is based on the finite-difference time-domain method, while Fig. 8 is based on the finite element analysis method. From the simulation results, we can get the fact that the magnetic field is symmetrical about the centroid but non-uniform.

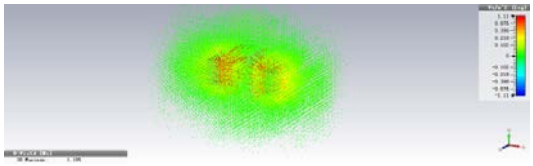

Fig.7 Side view of the magnetic induction intensity of permanent magnets

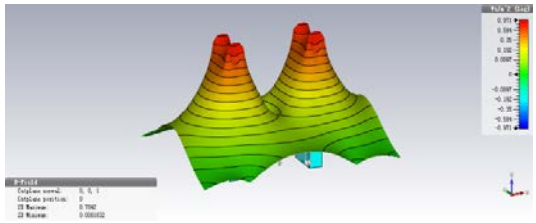

Fig. 8 Top view of induction intensity of permanent magnets

3.2 Simulation Of The Magnetic Field Of The Focusinging Coil

There is only one group of focusing coil in the two-dimensional actuator which controls the movement of the movable parts in the Y direction. Using coil excitation method in the CST software, the magnetic field distribution of the focusing coil can be simulated and calculated. The required simulation parameters are the current and turns which are shown in the Table 2:

Table 2 Parameters of focusing coil

current(A)	turns
0.3	56

The spatial magnetic induction intensity distribution of the focusing coil is shown in Fig. 9 and 10. It is apparent that the distribution of the focusing coil is symmetrical about the centroid but non-uniform, which is similar to the distribution of the tracking coil. Moreover, the magnetic induction is much smaller than that of the permanent magnet.

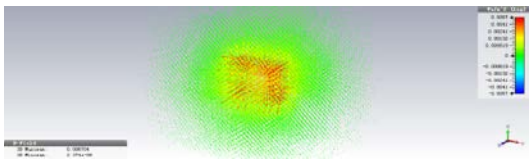

Fig. 9 Side view of the magnetic induction intensity of the focusing coil

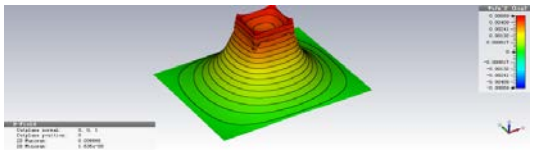

Fig. 10 Top view of induction intensity of the focusing coil

3.3 Simulation Of The Tracking Coil Magnetic Field

Tracking coils of the actuator are divided into four groups. They are distributed on the sides of focusing coil. The parameters needed are the current and turns are shown in the Table 3.

Table 3 Parameters of tracking coil

current (A)	turns
0.3	4*23

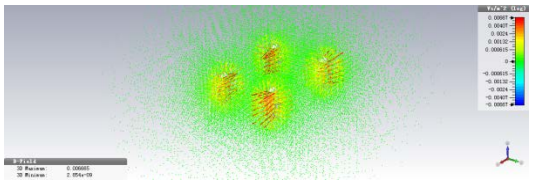

Fig.11 Side view of magnetic induction intensity of the tracking coil

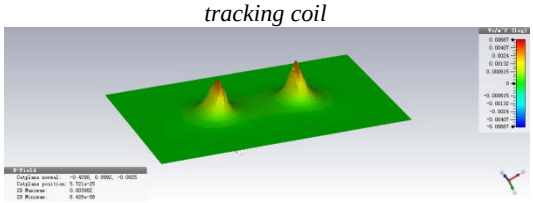

Fig.12 Top view of induction intensity of the tracking coil

The spatial magnetic induction intensity distribution of the tracking coil is shown in Fig. 11 and 12. The total spatial distribution of magnetic field of the actuator can be obtained through similar analysis as shown in Fig. 13 and 14.

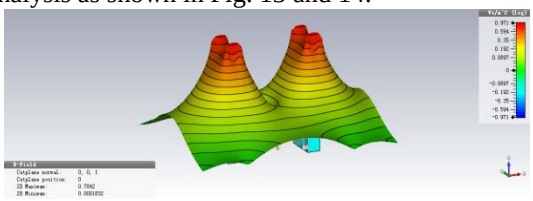

Fig.13 Synthesize overall induction intensity of the actuator

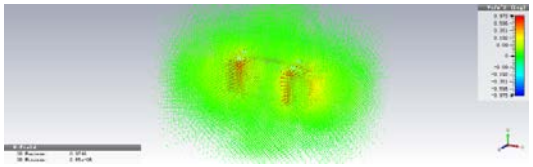

Fig.14 Side view of the overall induction intensity

Journal of Theoretical and Applied Information Technology
30th April 2013. Vol. 50 No.3

ISSN: 1992-8645 www.jatit.org E-ISSN: 1817-3195

Through the simulation, it can be concluded that the magnetic field of the actuator is symmetric to the center of the actuator but non-uniform. When the movable parts move in the non-uniform magnetic field, they deviate from the center position. The movable part is not only actuated in the expected direction, but also is forced in another direction caused by the asymmetric magnetic field, which result in a crosstalk movement.

4 . INFLUENCE OF STRUCTURAL PARAMETER OF ACTUATOR ON THE MAGNETIC FIELD

It has been shown that magnetic field of actuator is generated by the permanent magnet, focusing coil and tracking coils. Some of their structure parameters such as the height of the permanent magnet and the width and thickness of focusing coil are the key parameters that should be considered while designing the actuator.

In order to verify the effect of the above structure parameters on the focusing and tracking motion, in the following, two segments that across the centroid and respectively parallel to the X axis and the Y axis are selected for analysis. The intensity of magnetic induction on the line is analyzed along with the varied structure parameters. The ranges of movement of the movable parts are $\pm 0.5mm$ for the focusing direction and $\pm 0.3mm$ for the tracking direction. The magnetic field variation is studied within this range of the two segments.

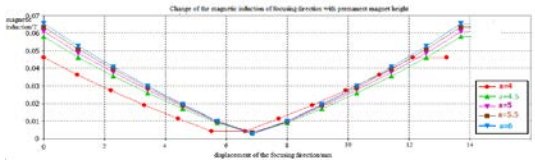

Fig.15 Change Of The Magnetic Induction Of Focusing Direction With Height Variation Of Permanent Magnet

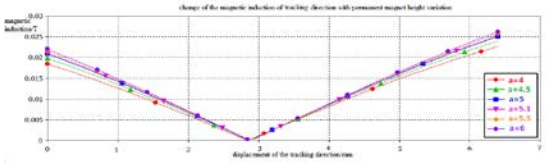

Fig.16 Change Of The Magnetic Induction Of Tracking Direction With Height Variation Of Permanent Magnet

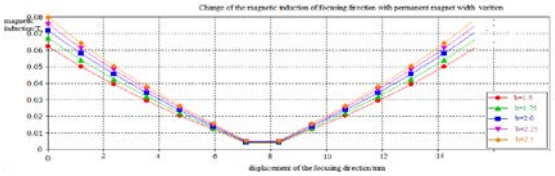

Fig.17 Change Of The Magnetic Induction Of Focusing Direction With Width Variation Of Permanent Magnet

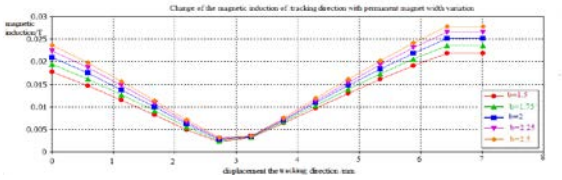

Fig.18 Change Of The Magnetic Induction Of Tracking Direction With Width Variation Of Permanent Magnet

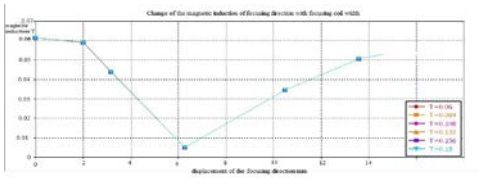

Fig.19 Change Of The Magnetic Induction Of Focusing Direction With Width Variation Of Focusing Coil

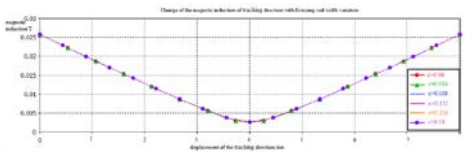

Fig.20 Change Of The Magnetic Induction Of Tracking Direction With Width Variation Of Focusing Coil

Based on the analysis results as shown in Fig 15 to 20, it can be concluded that the magnetic field distribution of the focusing direction and the tracking direction will be more uniform when the height or thickness of the permanent magnet is reduced. Crosstalk characteristic in the actuator will be then weakened. However, the thickness change of the focusing coil has little effect on the magnetic field distribution both on the focusing direction or the tracking direction. For example, considering the minimum electromagnetic force that required to drive the moveable parts of the actuator, the magnetic induction should, respectively, be greater than $0.055T$ in the focusing direction and $0.017T$ in the tracking direction, then the optimal structure parameters can be obtained with the height of the permanent magnetic a =4.5mm and the width of the permanent magnetic b =1.75mm. The influence of the width change of the focus coil is little.

5. CONCLUSION

In this paper, the distribution properties of the actuator spatial magnetic field is analyzed and simulated by the CST software based on FDTD principle. The essential cause of the crosstalk characteristic in the actuator is investigated. Through simulation, the trends of the magnetic induction variation in the focusing and tracking direction with the change of actuator structure parameters including the height, the thickness of the

ISSN: 1992-8645 www.jatit.org E-ISSN: 1817-3195

permanent magnet and thickness of the focusing coil are obtained, thus, based on which the desired structure parameters of the actuator are optimized. Since the crosstalk characteristic cannot be eliminated completely, an advanced control method for the pickup actuator is also expected in order to eliminate the crosstalk characteristic completely in the next generation high-density optical storage systems.

ACKNOWLEDGMENT

This work was supported by the National Natural Science Foundation of China (51075254), the Shanghai Pujiang Program (11PJ1404000) and the Innovation Program of Shanghai Municipal Education Commission (11YZ16).

REFRENCES:

[1] N. Park, Y. Park, K. Park, H. Yang. "Application of Next Generation Optical Data Storage Technologies", *IEEE Transactions on Magnetic*, Vol. 47, No. 3, 2011, pp.539-545.

[2] T. Shi, G. Wu, "Research on the focus servo system of DVD", China, April, 2008, pp.15-20.

[3] S.S. Wang, "Research on optic pickup adjusting machine digital servo system of DVD", China, February, 2006, pp.23-25.

[4] H.D. Kwon, and Y.P. Park, "Dynamic characteristics of stepped cantilever beams connected with a rigid body", *Journal of Sound and Vibration*, 2003, Vol. 255, No. 4, pp. 701-717.

[5] H.H. William, A.B. John. Engineering electromagnetics, McGraw-Hill Science, Beijing, 2004.

[6] I.H. Choi, S.P. Hong, W.E. Chung et al. "Concentrated Anisotropic Magnetization for High Sensitivity of Optical Pickup Actuator", *IEEE Transactions on Magnetics*, Vol.35, 1999, pp.1861-1864.

[7] B.Q. Zhang, J.S. Ma, L.F Pan, J.G. Ru, "Improvement of high frequency dynamic performance of actuator in optical pickup by finite element and sensitivity methods", *Optics and Precision Engineering*, Vol. 15, No.7, 2007, pp.1002-1008.